

# ON LATENT INFECTION AND DRUG RESISTANCE IN HIV PHARMACODYNAMICS

KAYLA ANDRUS AND AUDREY OLIVER

ABSTRACT. Highly active antiretroviral therapy (HAART) has been successful in controlling HIV replication for numerous patients. The effectiveness of HAART may be dependent on a multitude of factors, such as pharmacodynamics of the drugs, latent infection, and drug-resistant virus. To understand the dynamics that each play in managing HIV, we create a mathematical model to explain observations of pharmacodynamics at the intersection of latent infection and drug-resistant virus. We use the model to study the effects drug-resistant HIV treated with enfuvirtide (ENF). Furthermore, we assess the viral invasion threshold for drug-sensitive and drug-resistant virus.

## 1. INTRODUCTION

Human Immunodeficiency Virus (HIV) is a major public health concern globally, with approximately 39 million people living with the virus and 40.4 million HIV-related deaths as of 2022. HIV targets the body's immune system, specifically the CD4+ T cells, which aim to help the immune system fight infections. For most HIV-infected patients, highly active antiretroviral therapy (ART) has successfully controlled viral replication, allowing for longer, healthier lives. However, HIV type 1 (HIV-1) persists in patients. This is due to two main factors: the rapid establishment of viral reservoirs, which harbor infection within resting CD4+ T cells, and patients' development of drug resistance, which is the creation of mutated cells that render the medication ineffective.

Viral reservoirs are comprised of cells or tissues that contain replication-competent HIV but remain dormant for long periods of time and do not actively replicate in their resting state. Resting CD4+ T cell infection (RCI) is described by the existence of these dormant, or latently infected, cells. The frequency of RCI is comprised of the following: (i) the entry of cells into the viral reservoir through direct infection of resting cells or the de-activation of active infectious cells; and (ii) the loss of cells from the viral reservoir through death or activation of infected resting cells. Due to the resting nature of these latently infected cells, ART medication, which targets the reproduction process of infectious viruses, has no destination unless the resting cells become active. The activation of cells within the viral reservoir occurs over unpredictable lengths of time. Thus, a barrier of treatment has formed in which HIV patients must take medication for their entire life span to avoid the risk of relapse. This latent reservoir,

---

*Date:* December 18, 2024.

while extremely small, is universal throughout HIV patients and poses the first of two great challenges in eradicating HIV infection.

Drug resistance in HIV patients occurs when the virus mutates and becomes less detectable to antiretroviral therapy, necessitating changes in the treatment regimen. This resistance poses a significant challenge in managing HIV, as it limits the available options for effective therapy and can lead to treatment failure. While attempts at directly targeting the mutated infectious cells have been unsuccessful, a recent study found that re-administration of drugs undergoing “virological failure,” i.e. an observable increase in viral load after the formation of drug resistance, may increase counts of healthy CD4+ T cells. Although this does not affect the viral load, it is beneficial to the patient by providing them with additional capable T cells, strengthening their immune system and lowering the risk of opportunistic infections or complications commonly associated with HIV.

There are five prominent categories of antiretroviral drugs used to treat HIV: nucleoside reverse transcriptase inhibitors (NRTI), nonnucleoside reverse transcriptase inhibitors (NNRTI), protease inhibitors (PI), fusion inhibitors (FI), and integrase inhibitors (II). Each type of ART drug interrupts the HIV life cycle at a different point in reproduction, and thus, each possesses a different and unique pharmacodynamic profile. Antiretroviral therapy incorporates drugs from all classes, involving combinations that most effectively suppress viral load.

Pharmacodynamics studies how drugs affect the body, focusing on which life cycle stage the drugs interrupt, the relationship between drug concentration and effect, and the course of drug action relative to time. Analyzing each drug’s unique pharmacodynamic profile, specifically the parameters of dose-response curve slope, the ratio of the maximum dosage to the 50% inhibitory concentration, the drug’s half-life, and the dosing interval, helps determine optimal dosing regimens and improve drug efficacy. Recent studies have shown, even, that early treatment using drugs with a good pharmacodynamic profile could postpone or prevent the establishment of viral infection. In this study, we aim to show the influence pharmacodynamics and timing of treatment have on creating regimens that could prevent latent reservoirs from forming, leading to the potential eradication of HIV for users.

Slope values are class-specific for antiviral drugs and define intrinsic limitations on antiviral activity for some classes. The drug’s dose-response curve shows the relationship between the drug concentration and its antiviral effect. Each class of antiviral drugs, such as NRTIs, NNRTIs, PIs, FIs, and IIs, has its characteristic slope value. This slope reflects how the drug’s efficacy changes with concentration. For example, a steeper slope indicates that small changes in drug concentration result in significant changes in antiviral activity, while a flatter slope suggests a more gradual response.

The maximum achievable effect for certain classes might be constrained by how the drug interacts with its target. For instance, some drugs may reach a plateau in efficacy

beyond which increasing the dose does not result in a proportional increase in antiviral activity.

Only agents with slopes  $> 1$  achieve high-level inhibition of single-round infectivity, a finding with profound implications for drug and vaccine development.

Inhibition at clinical concentrations can only be predicted from IC50 if the shape of the dose-response curve is also known. The curve shape is influenced by cooperative interactions and is described mathematically by the slope parameter or Hill coefficient ( $m$ ).

In this study, we developed a mathematical model that incorporates the most prominent challenges and promising developments in HIV eradication research: viral reservoirs, drug resistance, and the involvement of pharmacodynamics in the creation of treatment regimens. The goal is to provide insights into overcoming these barriers and enhancing treatment strategies, with the overall objective of contributing to the development of a remedy for HIV.

## 2. MODEL

**2.1. DRPLHI Model.** We derive a drug-resistant pharmacodynamic latent HIV Infection (DRPLHI) model by incorporating time-varying efficacy of ART in a model of latent and drug-resistant viral dynamics. A schematic diagram of the model is shown in Figure 1.

As in previous models, we consider three mutually exclusive compartments: uninfected target cells ( $T$ ), productively infected drug-sensitive cells ( $I_s$ ), and productively infected drug-resistant cells ( $I_r$ ). Following a pharmacodynamic latent infection model, we consider two compartments for latently infected drug-sensitive cells ( $L_s$ ) and latently infected infected drug-resistant cells ( $L_r$ ). We further consider two compartments to measure free drug-sensitive virus ( $V_s$ ) and drug-resistant virus ( $V_r$ ). We describe the dynamics using the following differential equations:

$$(2.1) \quad \frac{dT}{dt} = \lambda - dT - \beta_s \Omega_{is}(t) V_s T - \beta_r \Omega_{ir}(t) V_r T, \quad T(0) = T_0,$$

$$(2.2) \quad \frac{dI_s}{dt} = (1 - f_s)(1 - \mu_s) \beta_s \Omega_{is}(t) V_s T + a_s(1 - \mu_s) L_s - \delta I_s, \quad I_s(0) = \frac{c_s}{p_s} V_s(0),$$

$$(2.3) \quad \frac{dI_r}{dt} = (1 - f_s) \mu_s \beta_s \Omega_{is}(t) V_s T + (1 - f_r) \beta_r \Omega_{ir}(t) V_r T + a_r L_r + a_s \mu_s L_s - \delta I_r, \quad I_r(0) = \frac{c_r}{p_r} V_r(0),$$

$$(2.4) \quad \frac{dL_s}{dt} = f_s \beta_s \Omega_{is}(t) V_s T - a_s \mu_s L_s - \delta L_s, \quad L_s(0) = L_{s0},$$

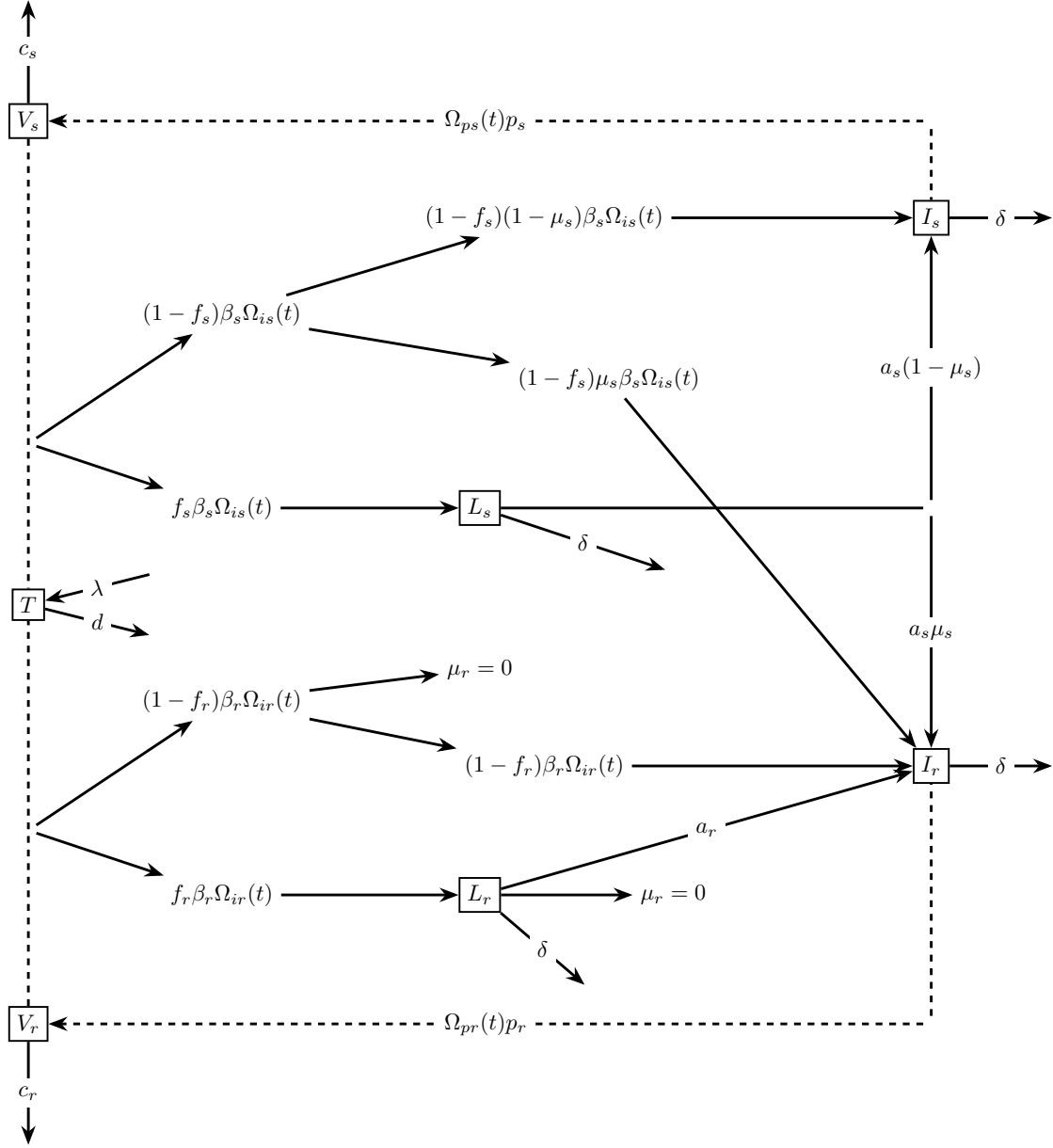


FIGURE 1. Schematic diagram of drug-resistant and drug-sensitive latent HIV infection.

$$(2.5) \quad \frac{dL_r}{dt} = f_r \beta_r \Omega_{ir}(t) V_r T - a_r L_r - \delta L_r, \quad L_r(0) = L_{r0},$$

$$(2.6) \quad \frac{dV_s}{dt} = \Omega_{ps}(t)p_s I_s - c_s V_s, \quad V_s(0) = V_{s0},$$

$$(2.7) \quad \frac{dV_r}{dt} = \Omega_{pr}(t)p_r I_r - c_r V_r, \quad V_r(0) = V_{r0}.$$

The target cells,  $T$ , are recruited at rate  $\lambda$  and die at rate  $d$ . Drug-sensitive virus infects target cells, where a fraction,  $f_s$ , become Drug-sensitive latently infected cells  $L_s$  at rate  $f_s\beta_s$ , while the remaining majority fraction,  $(1 - f_s)$ , become productively infected cells  $I_s$  at rate  $(1 - f_s)\beta_s$ .

Due to forward mutations at rate  $\mu_s$  during reverse transcription of viral RNA to DNA, a portion of productively infected cells become productively infected drug-resistant cells  $I_r$  at rate  $(1 - f_s)\mu_s\beta_s$ , while the remaining fraction  $(1 - \mu_s)$  productively infected drug-sensitive cells  $I_r$  at rate  $(1 - f_s)(1 - \mu_s)\beta_s$ . Drug-sensitive latently infected cells become activated at rate  $a_s$ , where a portion become productively infected drug-resistant cells at rate  $a_s\mu_s$ , and the remaining become productively infected drug-sensitive cells at rate  $a_s(1 - \mu_s)$ .

Similarly, infection of  $I_r$  and  $L_r$  by drug-resistant virus occurs at a reduced infectivity rate  $\beta_r = (1 - \alpha)\beta_s$ , where  $\alpha$  is the fitness cost of the mutant virus, i.e., the reduction of the infectivity of the resistant virus compared to the wild-type (sensitive) virus. A fraction  $f_r$  become latently infected  $L_r$  at rate  $f_r\beta_r$ , while the remaining fraction  $(1 - f_r)\beta_r$ , become productively infected cells  $I_r$  at rate  $(1 - f_r)\beta_r$ . From a previous model, it is observed that the loss of resistant virus due to backward mutation is negligible, and the fitness cost plays a more important role. Therefore, we assume no backward mutation ( $\mu_r = 0$ ) for our model. Hence, drug-resistant latently infected cells become drug-resistant productively infected cells at rate  $a_r$ . Drug-resistant and sensitive latently and productively infected cells die at rate  $\delta$  and produce new virions at rate  $p$ . Drug-sensitive and drug-resistant virions are cleared at rates  $c$ .

Different classifications of drugs used in ART effect different parts of the HIV life cycle. they either reduce the infection rate  $\beta$  of  $T$  cells, or the production rate of virus  $p$ . It is found that the mutations of productively infected cells alter drug-specific parameters. Therefore, we denote the effects of ART separately for drug sensitivity and drug resistance. During ART, time-varying residual viral infectivity of both productively and latently infected drug-sensitive cells reduce the infection rate by  $\Omega_{is}(t)$ . In contrast, the drug-resistant are reduced by  $\Omega_{ir}(t)$ . Time-varying residual viral production during ART reduces the production rate by  $\Omega_{ps}(t)$  and  $\Omega_{pr}(t)$  for infected drug-sensitive and drug-resistant virions, respectively. The effectiveness of drugs are given by  $\epsilon_i(t) = 1 - \Omega_i(t)$  and  $\epsilon_p(t) = 1 - \Omega_p(t)$ .

**2.2. Pharmacodynamics incorporation.** Following a classical dose-response, the residual viral infectivities,  $\Omega_{is}(t)$  and  $\Omega_{ir}(t)$ , and the residual viral productions,  $\Omega_{ps}(t)$  and  $\Omega_{pr}(t)$ , during ART are formulated as follows:

$$\begin{aligned}
 \Omega_{is}(t) &= \frac{1}{1 + [D_{is}(t)/ED_{50}^{is}]^{m_{is}}}, \\
 \Omega_{ir}(t) &= \frac{1}{1 + [D_{ir}(t)/ED_{50}^{ir}]^{m_{ir}}}, \\
 \Omega_{ps}(t) &= \frac{1}{1 + [D_{ps}(t)/ED_{50}^{ps}]^{m_{ps}}}, \\
 \Omega_{pr}(t) &= \frac{1}{1 + [D_{pr}(t)/ED_{50}^{pr}]^{m_{pr}}}.
 \end{aligned}
 \tag{2.8}$$

The plasma concentration of drugs required for 50% maximal effect are denoted by  $ED_{50}^{is}$ ,  $ED_{50}^{ir}$ ,  $ED_{50}^{ps}$ , and  $ED_{50}^{pr}$ . Hill's coefficients are represented by  $m_{is}$ ,  $m_{ir}$ ,  $m_{ps}$ , and  $m_{pr}$ . Time-varying plasma concentrations of drugs,  $D_{is}(t)$ ,  $D_{ir}(t)$ ,  $D_{ps}(t)$  and  $D_{pr}(t)$  are as follows:

$$\begin{aligned}
 D_{is}(t) &= D_{max}^{is} e^{-k_{is}(t-t_j)}, \\
 D_{ir}(t) &= D_{max}^{ir} e^{-k_{ir}(t-t_j)}, \\
 D_{ps}(t) &= D_{max}^{ps} e^{-k_{ps}(t-t_j)}, \\
 D_{pr}(t) &= D_{max}^{pr} e^{-k_{pr}(t-t_j)}. \\
 t_j \leq t < t_{j+1}, \quad j &= 0, 1, 2, \dots
 \end{aligned}
 \tag{2.9}$$

Drug intake interval is represented by  $\Delta t = t_{j+1} - t_j$ , decay slopes of the drug concentrations are  $k_{is}$ ,  $k_{ir}$ ,  $k_{ps}$ , and  $k_{pr}$ , and the drug concentrations administered at intake are denoted by  $D_{max}^{is}$ ,  $D_{max}^{ir}$ ,  $D_{max}^{ps}$ , and  $D_{max}^{pr}$ .

To assess our model, we use data from previous studies for initial conditions and beginning parameters. Given their focus on ENF and the V38A mutant virus, we utilize ENF and V38A drug-specific parameters for the sensitivity and perform varying simulations utilizing the SciPy package in Python.

### 3. REPRODUCTION NUMBER

It is common practice to calculate the basic reproductive number,  $R_0$ , to assess the infectivity of the virus. This calculation yields the average number of virus particles produced by a single virus particle. This is key to understanding whether a virus is infectious ( $R_0 < 1$ ) or will die out ( $R_0 > 1$ ). While  $R_0$  helps to understand the drug efficacy at the beginning of infection, the effective reproductive number  $R_e$  essentially measures the  $R_0$  introduced at time  $t$  into the infection cite. This helps to understand

the viral growth later during infection. To address the limitations of both  $R_0$  and  $R_e$ , we derive a viral invasion threshold under ART,  $R_i$ , guided from approaches from Wang and Zhao, Liu, Zhao, and Zhao, and Vaidya and Wahl. We follow these approaches for the viral invasion threshold of three different cases: drug-resistant viral invasion threshold ( $R_{i1}$ ), drug-sensitive viral invasion threshold ( $R_{i2}$ ) with no forward mutation  $\mu_s = 0$ , and drug-sensitive viral invasion threshold ( $R_{i3}$ ) with forward mutation  $\mu_s \neq 0$ .

To observe the effects of drug parameters on the viral invasion threshold  $R_i$ , we use  $R_i$  as a function of the dose response curve, drug half-life, ratio of drug dosage to 50% inhibitory concentration, and drug intake interval. For  $R_{i1}$ , we further consider fitness cost, as this is an important factor for drug-resistant virus. We alter the respective drug-specific parameters for drug-resistance and drug-sensitivity for the three  $R_i$  cases, and remaining base values follow V38A parameters.

3.0.1. *Ri 1.* We first observe the viral invasion threshold for drug-resistant virus,  $R_{i1}$  (Fig. 2). We find that  $R_{i1}$  decreases as the pharmacodynamic parameters for the max drug dose administered, half-life, and slope of the given drug increase. Increases in these parameters indicate more drug administered, and longer lasting effects in the body, therefore decreasing the reproducibility of the drug-resistant virus. In the case of increasing the dose interval,  $R_{i1}$  increases. This is due to longer time spans between the drug being administered, and there no longer being drug available in the body to inhibit reproduction of the virus.

As fitness cost increases,  $R_{i1}$  decreases. The fitness cost inversely effects the infection rate of drug-resistant virus, where higher fitness costs result in lower infection rates. Therefore the viral invasion threshold decreases.

3.0.2. *Ri 2.* We also observe the viral invasion threshold for drug-sensitive virus,  $R_{i2}$ , with no forward mutation [Fig. 3]. In other words, we observe with no presence of drug resistant virus.  $R_{i2}$  follows the same trends as  $R_{i1}$  for all changes to pharmacodynamic parameters. Fitness cost is not considered since there is no presence of drug-resistant virus.

3.0.3. *Ri 3.* In the third case,  $R_{i3}$ , we consider the presence of forward mutation on the viral invasion threshold for drug-sensitive virus [Fig. 4]. We find that with the presence of drug-resistant virus, the viral invasion threshold for drug-sensitive virus remains low, since the amount of T cells decreases drastically. Therefore, it requires extreme parameter values for fitness cost and fold change to observe differences in  $R_{i3}$ . Higher fitness cost correlates to a lower infection rate of drug-resistant cells, leading to higher production of T cells, resulting in higher  $R_{i3}$ . Similarly, a higher fold change indicates a higher  $ED_{50}^{ir}$ , resulting in higher plasma concentration of drugs necessary for 50% maximal effect. This leads to higher production of T cells and higher  $R_{i3}$  overall.

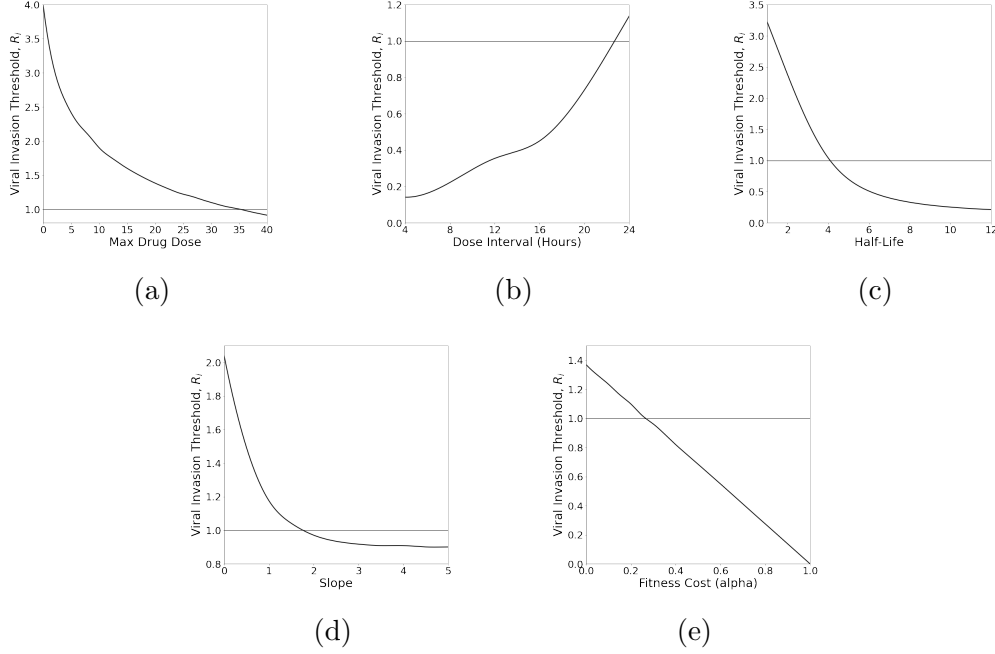


FIGURE 2. The viral invasion threshold for case 1 resistant virus,  $R_i1$ , as a function of (a) the slope of dose-response curve,  $m$ , (b) the half-life of drugs,  $t_{1/2}$ , (c) the ratio of the maximum doses to the 50% inhibitory concentration,  $D_{\max}/ED_{50}$ , (d) the dosing interval,  $\tau$ , and (e) fitness cost. In each case, remaining pharmacodynamic parameters were fixed at their base value, i.e.,  $D_{\max}/ED_{50} = 30$ , half-life  $t_{1/2} = 3.8$  hours, dosing interval  $\tau = 1$  day,  $m = 1.12$ ,  $\alpha = 0.17$ . The other viral dynamic parameters are listed in Table 1.

## 4. RESULTS

**4.1. Enfuvirtide Pharmacodynamics.** To observe the dynamics of our model, we incorporate drug Enfuvirtide, and its respective drug-resistant parameters. When drug is administered, we note a decline in virus and latently infected cells over time [Fig. 5a and 5b]. This is expected as the drugs begin to control the virus. Additionally, resistant virus and infected cells begin to overtake the sensitive virus and infected cells, since the drug cannot properly control the drug-resistant virus and infected cells due to the changes in parameters. We further explore the impact of changes in pharmacodynamic parameters of drug-resistance on outcomes in the next section.

Additionally, as virus and infected cells decrease, the CD4 count (summation of infected cells and T cells) also decrease [Fig. 6a]. However, it is important to note that



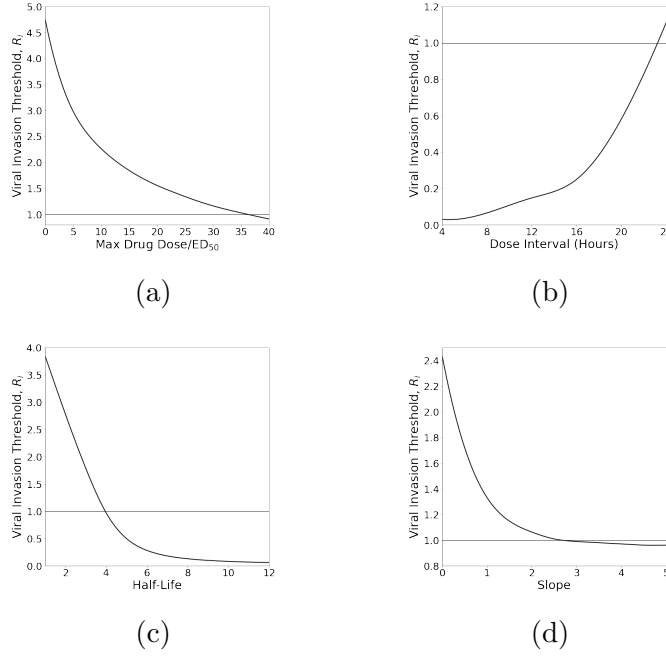


FIGURE 3. The viral invasion threshold for case 2 sensitive virus,  $R_i$ , as a function of (a) the slope of dose-response curve,  $m$ , (b) the half-life of drugs,  $t_{1/2}$ , (c) the ratio of the maximum doses to the 50% inhibitory concentration,  $D_{\max}/ED_{50}$ , and (d) the dosing interval,  $\tau$ . In each case, remaining pharmacodynamic parameters were fixed at their base value, i.e.,  $D_{\max}/ED_{50} = 30$ , half-life  $t_{1/2} = 3.8$  hours, dosing interval  $\tau = 1$  day,  $m = 1.12$ ,  $\alpha = 0.17$ . The other viral dynamic parameters are listed in Table 1.

this is mostly attributes of the sensitive and resistant-infected cells. While infection remains low, the T cells begin to increase [Fig. 6b].

**4.2. Visual Plots.** In this study, we focused on several pharmacodynamic variables and analyzed their impact on latent virus, resistant virus, and CD4 count, among other results. Each of the plots varies fitness cost on the y-axis, which represents the degree to which the virus is hindered from reproducing and surviving due to genetic mutations that may occur. A resistant strain with a higher fitness cost (higher  $\alpha$ ) is less efficient in transmitting and establishing itself in the population than a sensitive strain. Additional variables on the x-axis include the maximum drug administered ( $d_{\max}$ ), the scaling factor for the mutated virus' change in half-maximal inhibitory concentration (IC50- quantifies the drug's ability to inhibit viral reproduction by 50%), and the scaling factor for the mutated virus' change in Hill's coefficient or slope ( $m$ -

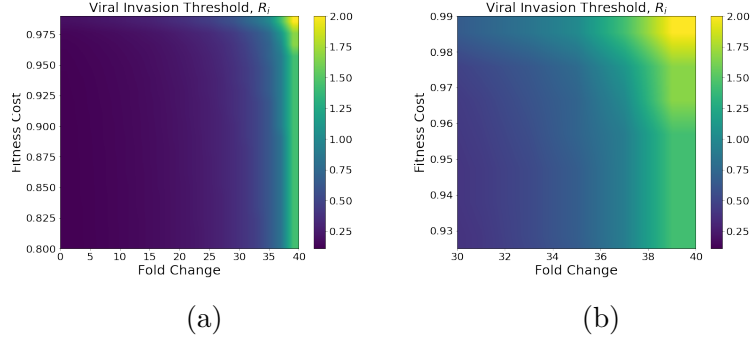


FIGURE 4. The viral invasion threshold for case 3 sensitive virus with forward mutation,  $R_i$  3, as a function of both fold change and fitness cost. Infection rate of drug-sensitive cells=  $4e-8$ .

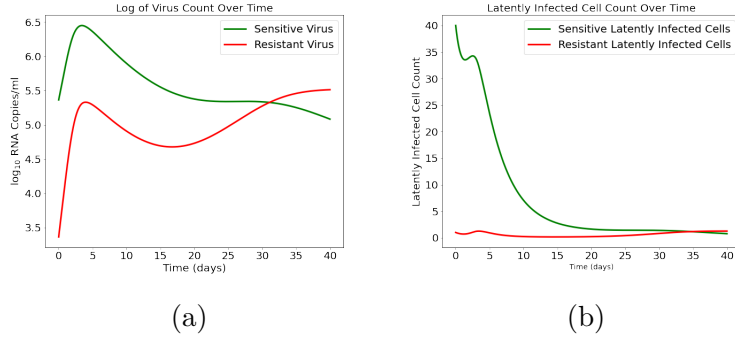


FIGURE 5. Virus and latently infected cells with early treatment

quantifies the steepness of the dose-response curve of the drug). With a focus on the effects of drug resistance and latently infected cells combined into one mathematical model, we aim to observe the outcomes of our model based on varying fitness costs and drug-specific parameters. In doing so, we can see the effects of resistance and latent infection simultaneously and their effect on each other. Additionally, the time post-initial infection at which treatment is initiated is shown to affect the control of viral load. Minimal weeks post-infection (WPI) or early treatment may lead to quicker control of HIV in patients versus beginning ART after the infection reaches a steady state (late treatment).

As previously stated, drug resistance drastically alters drug-specific parameters, more specifically fractional changes in Hill's coefficients ( $m_i$  and  $m_p$ ), and fold changes in the plasma drug concentrations for 50% maximal effect ( $ED_{50}^i$  and  $ED_{50}^p$ ). Therefore, we run simulations of varying fitness cost against varying fractional changes of  $m_i$  and  $m_p$ , and fold changes of  $ED_{50}^i$  and  $ED_{50}^p$ , for early treatment and late treatment.

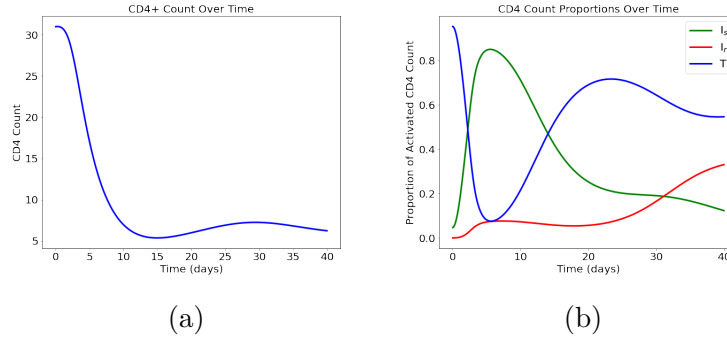


FIGURE 6. CD4 count (left) and the corresponding proportions of contribution (right) from infected sensitive cells (green), infected resistant cells (red), and T cells (blue).

We take early treatment to be 0 WPI and late treatment at 52 WPI and run each simulation for one year, once treatment is initiated, to see the long-term outcomes of each combination of parameters.